Volume 5 Issue 1 (March 2025)
DOI 10.24191/jaeds.v5i1.103
eISSN 2805-5756

Journal of Applied Engineering Design & Simulation

Formability Analysis of Dissimilar Aluminium Tailor Welded Blanks by Low-Powered Fibre Laser for Lightweight Automotive Application

Mohd Fadzil Jamaludin[1,2], Ahmad Baharuddin Abdullah[1,*], Zahurin Samad[1] and Farazila Yusof[2,3,4]
[1]Metal Forming Research Lab, School of Mechanical Engineering, Universiti Sains Malaysia, Nibong Tebal, 14300, Pulau Pinang, Malaysia.
[2]Centre of Advanced Manufacturing and Material Processing (AMMP Centre), Faculty of Engineering, Universiti Malaya, 50603, Kuala Lumpur, Malaysia.
[3]Department of Mechanical Engineering, Faculty of Engineering, Universiti Malaya, 50603, Kuala Lumpur, Malaysia.
[4]Centre for Foundation Studies in Science, Universiti Malaya, 50603, Kuala Lumpur, Malaysia.
[*]corresponding author: mebaha@usm.my

ABSTRACT

The automotive industry is increasingly adopting lightweight materials to improve fuel efficiency and reduce emissions, with aluminium alloys emerging as a promising option for vehicle weight reduction. This study investigates the formability challenges of dissimilar AA5052-H32 and AA6061-T6 aluminium tailor welded blanks (TWBs) fabricated using low-powered fibre laser welding for potential lightweight automotive applications. Welding parameters included laser powers of 270 W, 290 W and 310 W, paired with welding speeds of 10 mm/s, 15 mm/s and 20 mm/s, to join the dissimilar alloy pair in a butt-weld configuration via successive double-sided welding. Limiting dome height (LDH) tests revealed that the TWBs achieved only 35-40% of base metal formability, with fracture strains below 0.1 for both major and minor deformations. The presence of porosity in the weld zone, including a softening region identified by microhardness testing, contributed to premature failure during formability testing. These findings highlight the challenges associated with forming operations involving low-power laser welded aluminium TWBs and necessitate further research to improve formability and address manufacturing constraints.

Keywords: Formability; Tailor Welded Blanks; Aluminium Alloys; Low-power; Laser Welding.

Nomenclature

e_1	Major strain
e_2	Minor strain
l_0	Initial length (mm)
w_0	Initial width (mm)
l_0	Final length (mm)
w_f	Final length (mm)

Abbreviations

TWB	Tailor welded blanks
LDH	Limiting dome height
HAZ	Heat affected zone
CW	Continuous wave
CGSA	Circle grid strain analysis
IMC	Intermetallic compounds
FLD	Forming limit diagram

1.0 INTRODUCTION

Increasingly stringent government regulations on fuel economy and emissions are compelling automakers to reduce vehicle weights and minimise carbon emissions. This drive towards sustainable transportation has accelerated the adoption of lightweight materials, with aluminium alloys emerging as a key contender [1, 2]. Aluminium alloys offer an attractive combination of low density, high strength-to-weight ratio, and good corrosion resistance, making them ideal for replacing traditional steel in automotive body structures [3, 4]. To further optimise weight reduction and enhance design flexibility, the automotive industry has embraced tailor

Received on 20.03.2025
Accepted on 16.04.2025
Published on 25.04.2025

welded blanks (TWBs). TWBs are fabricated by joining two or more sheets of different materials, thicknesses, or coatings to create a single, composite blank [5, 6]. This approach allows for strategic material placement, enabling enhanced load distribution, reduced material usage, and tailored strength properties within a single component.

Low-powered fibre laser welding presents a promising method for producing aluminium TWBs for automotive applications [7, 8]. This welding technique offers several advantages over traditional methods. It minimises heat input, resulting in less distortion and a narrower heat-affected zone (HAZ). The narrow HAZ is particularly beneficial for maintaining material integrity and avoiding undesirable microstructural changes that can adversely affect mechanical properties. Moreover, low-power laser welding provides excellent precision and control, making it well suited for automated production processes. However, despite these advantages, the use of low-power laser welding to fabricate aluminium TWBs presents specific challenges related to formability. Formability, the material's ability to deform without failure, is critical for achieving complex shapes during stamping operations [11, 12].

Previous studies have explored the influence of welding processes on formability in various materials. Research on TWBs have shown that the presence of the weld zone can significantly reduce formability compared to monolithic materials [13, 14]. The weld zone often acts as a stress concentrator, leading to premature failure during forming operations. Additionally, investigations into weld defects, such as porosity, have found that these imperfections can markedly reduce the strain capacity of the welded blanks [15].

This study investigates the formability and behaviour of aluminium TWBs fabricated using low-powered fibre laser welding, focusing on the effects of laser power and welding speed on the formability of dissimilar AA5052-H32 and AA6061-T6 aluminium alloys. The aim is to provide valuable insights into the challenges and opportunities associated with employing low-power laser welding for the production of lightweight automotive components. The findings will highlight the need for further research to improve the formability of these welded blanks and to address manufacturing constraints for wider industrial adoption.

2.0 METHODOLOGY

2.1 Material selection and welded specimen preparation

AA5052-H32 and AA6061-T6 aluminium sheet materials, with thicknesses of 1.5 mm and 1.0 mm, were procured from a local supplier. Rectangular specimens (100 mm x 50 mm) were prepared using a hydraulic shearing machine and categorised into two groups:

- Group A: Similar thickness (1.0 mm) for both AA5052-H32 and AA6061-T6
- Group B: 1.5 mm thickness for AA5052-H32 paired with 1.0 mm thickness for AA6061-T6.

Welding experiments were conducted using a low-power fiber laser welding system (StarFiber 300, ROFIN Baasel Lasertech) operating in continuous wave (CW) mode. The system featured a 1070 nm wavelength fibre laser with a maximum power output of 314 W. Double-sided butt welds, schematically shown in Fig. 1, were performed to ensure full penetration and minimise defects, with laser power ranging from 270 W to 310 W and welding speeds of 10-20 mm/s. Table 1 outlines the design of experiment for both Group A and Group B specimens.

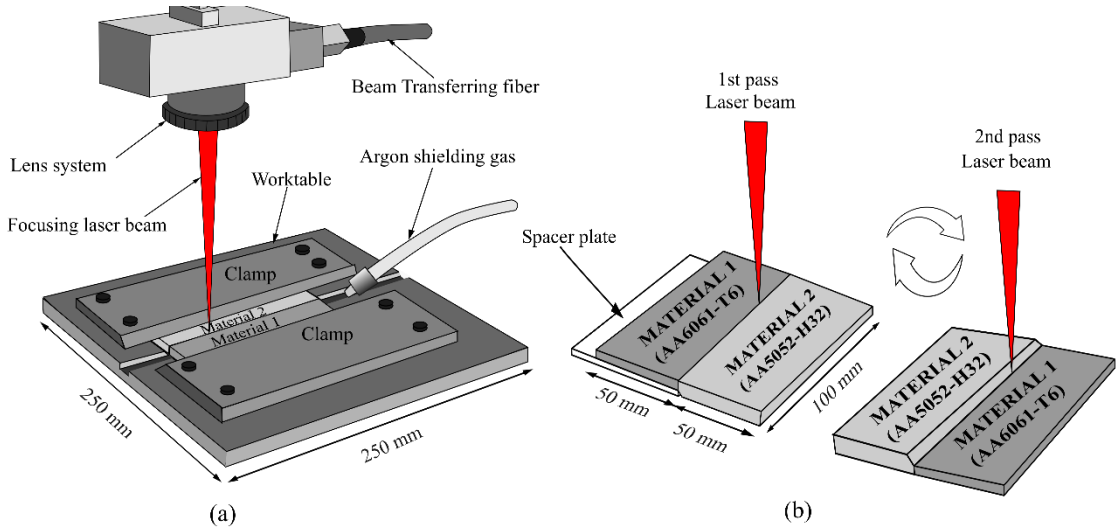

Figure 1. Schematic of the double-sided butt weld for welding of aluminium specimen pair showing a) apparatus set-up, and b) successive double-sided welding

Table 1: Design of experiments for welded specimen preparation for Group A and Group B

Specimen No	Welding Speed (mm/s)	Laser Power (W)	Group A	Group B
1	10	270	AA5052	AA5052
2	10	290	(1.0mm) –	(1.5mm) –
3	10	310	AA6061	AA6061
4	15	270	(1.0mm)	(1.0mm)
5	15	290		
6	15	310	Different	Different
7	20	270	alloy, similar	alloy, different
8	20	290	thickness	thickness
9	20	310		

2.2 Limiting Dome Height (LDH) Test

The LDH test was conducted to evaluate the formability of the TWB specimens. A customised LDH test setup was mounted on a universal testing machine (Instron UTM, model 3369). The setup comprised a hemispherical punch and a die featuring a mid-plate and locking bead mechanism for securely clamping the specimen, as shown in Fig. 2. During the test, the weld specimen was positioned over the mid-plate of the die, ensuring that the weld line was centrally aligned with the punch axis. For specimens with different thicknesses, a half-circular metal shim was employed to ensure uniform clamping pressure. The LDH test was initiated by applying a constant compression speed of 0.1 mm/s to the top plate, lowering the clamped assembly onto the punch. The test continued until fracture occurred in the specimen, indicating the maximum dome height achievable. Both the dome height and the load at fracture were subsequently recorded.

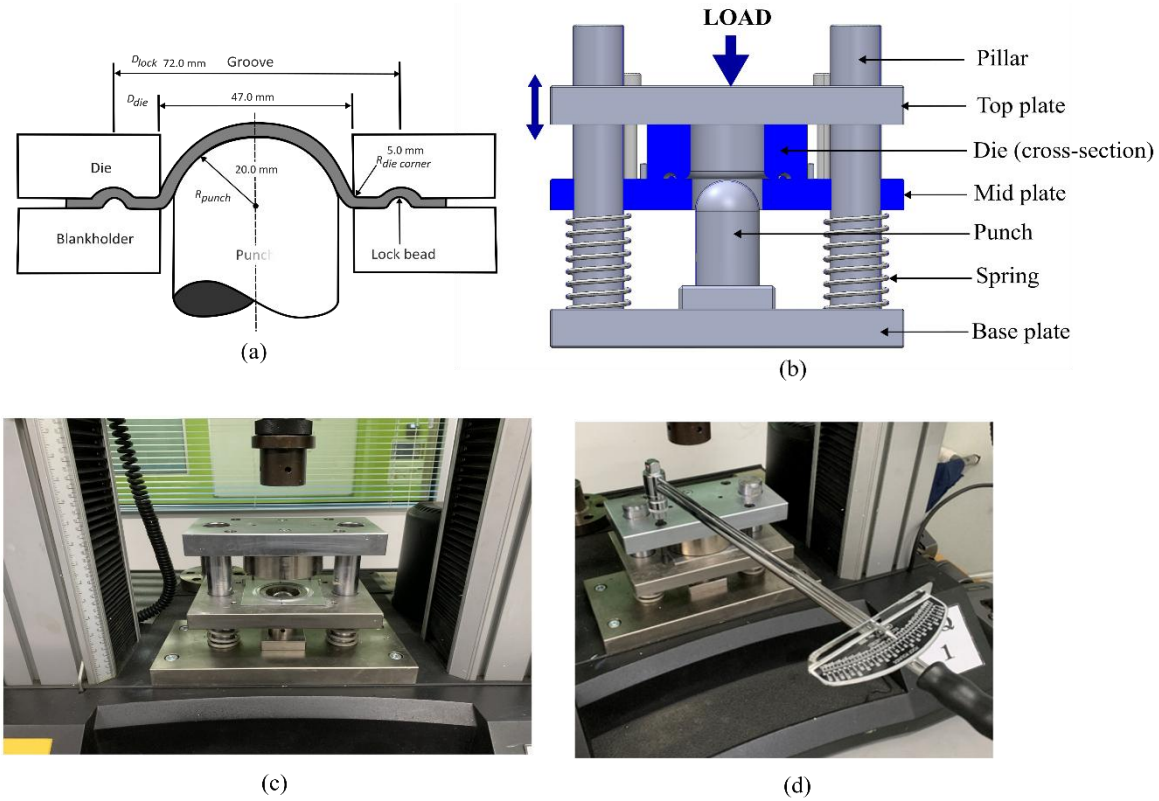

Figure 2. Limiting Dome Height (LDH) test apparatus showing a) schematics of the test, b) details of the LDH, c) set-up in UTM and d) securing the specimen using a torque wrench

2.2 Circle Grid Strain Analysis (CGSA)

To analyse the strain distribution at failure during the LDH test, a circle grid pattern was laser-etched onto the specimen surface before testing, as shown in Fig. 3. The circular grids were designed to enable measurement of the major and minor strains at the failure point and other locations on the dome.

After the LDH test, the deformed circle grid patterns were measured using image processing software. The major and minor strains, e_1 and e_2, were calculated based on the changes in the circle's dimensions (length and width) using Equation (1) and Equation (2), respectively.

$$\text{Major strain} = e_1 = \frac{l_f - l_0}{l_0} \times 100 \quad (1)$$

$$\text{Minor strain} = e_2 = \frac{w_f - w_0}{w_0} \times 100 \quad (2)$$

where l_0 is the initial length (mm), w_0 is the initial width (mm), l_f is the final length (mm) and w_f is the final width (mm).

The calculated major and minor strains were plotted to create a forming limit diagram (FLD), which provides a visual representation of the material's formability under different strain conditions.

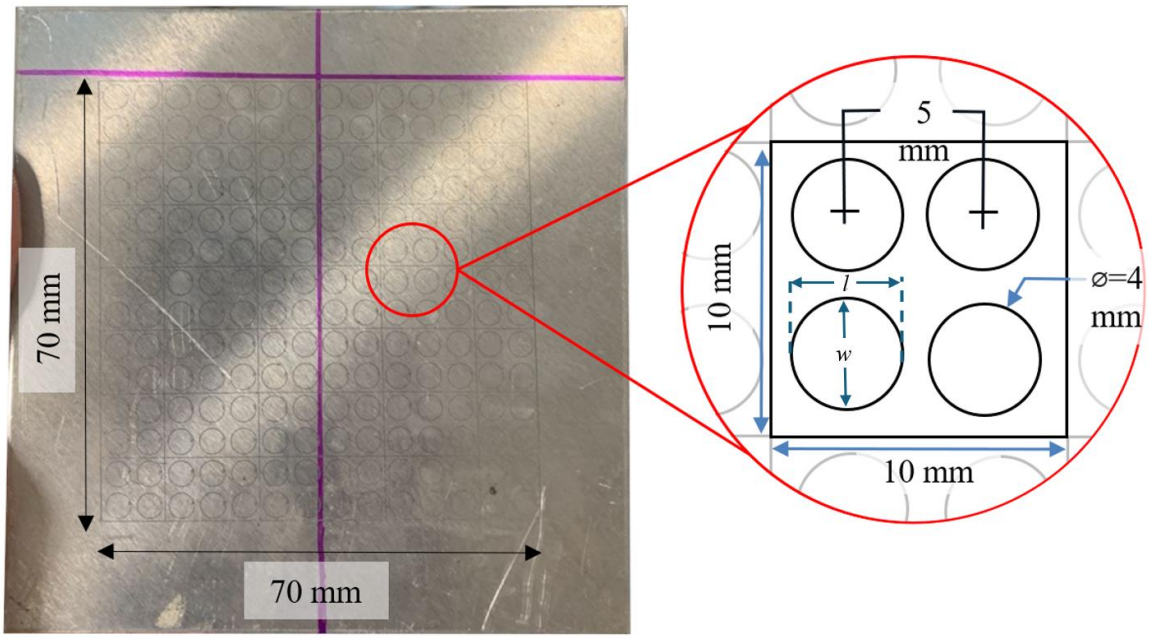

Figure 3. Laser-etched circular grids marked on the aluminium specimen

2.3 Microstructure and microhardness evaluations

Microstructural analysis using optical microscopy was performed to assess weld quality and identify defects. These methods assist in determining the depth of penetration, fusion zone morphology, the presence of porosity, and the distribution of alloying elements in the weld zone. The microhardness testing was conducted to assess the hardness profile across the weld region, heat-affected zone, and base material. This involved using a micro-Vickers hardness tester (HMV-2T, Shimadzu, Japan) to create an indentation on the specimen surface and measure the diagonal length of the indentation. A test force of 0.98 N and a dwell time of 10 s were chosen for the microhardness test.

3.0 RESULTS AND DISCUSSION

Figs. 4 and 5 show a tested LDH specimen, illustrating the formation of the dome-shaped extrusion and noting the location of failure. The corresponding results of LDH tests for the welded specimens are presented in Table 2, along with the LDH value for the base materials in Table 3.

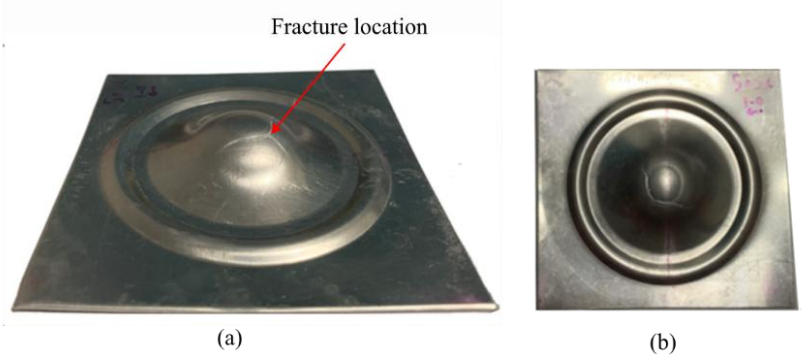

Figure 4. LDH tested specimen showing a) isometric view and b) top view

Figure 5. Cross-section of the LDH tested specimen showing the dome height at fracture

Table 2: Limiting Dome Height (LDH) results

Specimen No	Welding Speed (mm/s)	Laser Power (W)	Average Dome Height (mm)	
			Group A	Group B
1	10	270	4.71	3.37
2	10	290	3.48	4.82
3	10	310	4.65	4.77
4	15	270	3.14	3.54
5	15	290	4.87	4.51
6	15	310	3.78	5.14
7	20	270	3.42	3.05
8	20	290	5.03	3.16
9	20	310	4.58	4.66

Table 3: Results of LDH for the base materials

	Dome Height (H) (mm)			
Base Material	H_1	H_2	H_{avg}	SD
AA5052-H32				
1.0 mm thickness	11.89	12.28	12.09	0.276
1.5 mm thickness	14.68	14.62	14.65	0.042
AA6061-T6				
1.0 mm thickness	12.78	12.35	12.57	0.304
1.5 mm thickness	13.08	12.98	13.03	0.071
Legend:				
H_1 = Replication 1				
H_2 = Replication 2				
H_{avg} = Average				

The LDH results clearly demonstrate a significant reduction in formability for the TWB specimens compared to the base materials. The dome heights achieved by the TWBs were approximately 35-40% of the dome heights for the base metals, indicating a substantial loss of formability. Circle grid strain analysis (CGSA) was performed on selected specimens from Groups A and B to determine the forming limits. The results of the CGSA are plotted in Fig. 6.

The failure limits for the welded specimens are significantly less than the limits of the base metal AA5052-H32 and AA6061-T6. For the base metals, AA6061-T6 has good formability but is generally less than AA5052-H32 due to its higher strength and effects of heat treatment. Early failure of the welded specimen can be due to the reduced strength as compared to the base materials, and welding defects such as porosity, cracks or incomplete fusion that act as stress concentrators and significantly reduce the formability of the welded sample. Issues such as ductility and formation of brittle phases in the heat-affected zone can also cause premature failure in the weld. The experimental analysis reveals that the forming limits exhibit a remarkably narrow range, with fracture occurring at strains ≤ 0.1 for both major and minor deformations. The imposed limitations greatly restrict the potential use of this technology for commercial applications. Therefore, it is advisable to undertake additional research to overcome this constraint.

The microhardness evaluations across the transverse cross section of the weld for selected specimens from Group A and B are shown in Figs. 7 and 8, respectively. The included microstructure figures also depict the overlapping of the double-sided weld and presence of porosity in the joint. In general, it can be seen that microhardness is significantly less than the hardness of both AA5052 and AA6061 base materials. The microhardness profile of the weld shows a decreasing gradient in microhardness values from the 6061 side towards the AA5052 side, with the lowest microhardness on the AA5052 side. The strength of aluminium welds can be inferred from their hardness values, as demonstrated by various studies. Hardness serves as a reliable indicator of the mechanical properties of welded joints, particularly in aluminum alloys, where different zones exhibit distinct hardness profiles that correlate with their strength. For instance, the softening heat-affected zone often shows the lowest hardness and strength, while the welded zone typically exhibits higher hardness and strength [16].

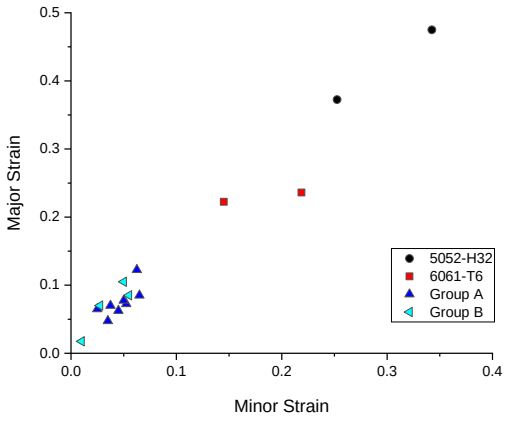

Figure 6. Minor strain-major strain plot showing points of failure

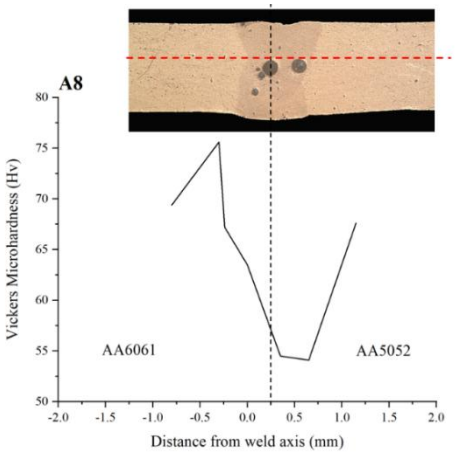

Figure 7. Microhardness distribution for specimen 8 (Group A)

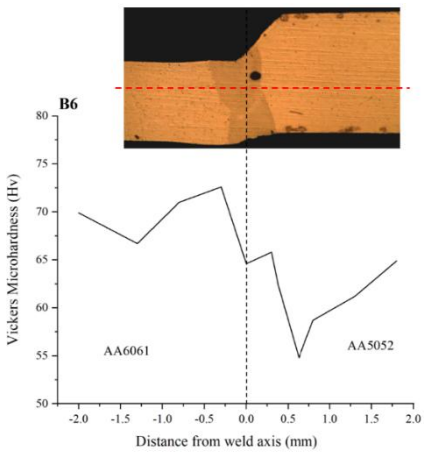

Figure 8. Microhardness distribution for specimen 6 (Group B)

This reduction in formability poses a significant challenge for the application of low-power laser welded aluminium TWBs in automotive sheet metal forming operations. Several factors can contribute to this reduced formability:

i. Weld Zone Microstructure: The weld zone, particularly the heat-affected zone (HAZ), exhibits a softened microstructure compared to the base materials [17]. This softening is attributed to the rapid heating and cooling cycles during laser welding, which can dissolve strengthening precipitates in the aluminium alloys, leading to a decrease in hardness and ductility. This reduced ductility in the HAZ limits the ability of the TWBs to withstand significant deformation during forming operations, leading to premature failure [18].

ii. Porosity: The presence of porosities within the weld zone act as stress concentrators, further weakening the joint and accelerating failure during forming [19, 20]. The formation of porosity in laser welding is often linked to the rapid solidification rates, which can trap gas bubbles within the molten metal. These gas bubbles can grow and coalesce during cooling, creating voids that reduce the load-bearing capacity and the formability of the welded joint [21].

iii. Intermetallic Compounds: The high cooling rates during laser welding can also lead to the formation of intermetallic compounds (IMCs) at the weld interface. While IMCs can sometimes improve strength, they can also be brittle and reduce the overall formability of the weld [22, 23]. The presence of IMCs in the weld zone can act as stress concentrators, particularly when subjected to bending or stretching forces during forming operations, leading to premature fracture [24]. However, in this article, the determination IMCs was not discussed.

iv. Dissimilar Alloy Combinations: The use of dissimilar aluminium alloys (AA5052-H32 and AA6061-T6) further complicates the formability of the TWBs. The different chemical compositions and microstructures of the alloys can lead to uneven heat distribution during welding, increasing the likelihood of defects and microstructural variations within the weld zone [25, 26].

4.0 CONCLUSION

This study investigated the formability of aluminium tailor welded blanks (TWBs) fabricated using low-powered fiber laser welding, focusing on dissimilar AA5052-H32 and AA6061-T6 aluminium alloys. While achieving full penetration with a double-sided welding strategy, the research revealed a significant reduction in formability compared to the base materials, which can severely limit the application of these TWBs in automotive sheet metal forming operations.

The limiting dome height (LDH) tests and circle grid strain analysis consistently demonstrated this reduced formability, with failure occurring at strains ≤ 0.1 for both major and minor strain deformations. This indicates a significantly limited strain capacity and highlights the need for further research to improve the formability of these TWBs.

The study attributes the reduced formability to a combination of factors including softening in the weld zone and the presence of porosities. The rapid heating and cooling cycles associated with laser welding led to a softened microstructure in the weld zone, particularly the heat-affected zone (HAZ), reducing the material's ductility. In addition, the presence of porosities in the weld zone act as stress concentrators, further weakening the joint and contributing to premature failure during forming.

ACKNOWLEDGEMENT

The first author gratefully acknowledges the scholarship support provided by the Ministry of Higher Education Malaysia, under the Hadiah Latihan Persekutuan (HLP) program. This work is funded by Geran Penyelidikan Pegawai Penyelidik MRUN (MROGS008-2024).

AUTHORS' CONTRIBUTION

Mohd Fadzil Jamaludin : Investigation, Validation, Writing – Original Draft
Ahmad Baharuddin Abdullah : Supervision, Conceptualization, Writing – Review & Editing
Zahurin Samad: Supervision, Conceptualization
Farazila Yusof: Methodology, Validation, Resources.

DECLARATION OF COMPETING INTEREST

The authors declare that they have no known competing financial interests or personal relationships that could have appeared to influence the work reported in this paper.

REFERENCES

[1] G. Refiadi, I.S. Aisyah, and J.P. Siregar, "Trends in Lightweight Automotive Materials for Improving Fuel Efficiency and Reducing Carbon Emissions," *Automotive Experiences*, vol. 2 no. 3, pp.78–90, 2019, doi: 10.31603/ae.v2i3.2984.

[2] S. Kleinbaum, C. Jiang, and S. Logan, "Enabling sustainable transportation through joining of dissimilar lightweight materials," *Mrs Bulletin*, vol. 44, no. 8, pp. 608–612, 2019, doi: 10.1557/MRS.2019.178

[3] Y. Gao et al., "Research progress, application and development of high performance 6000 series aluminum alloys for new energy vehicles," *Journal of Materials Research and Technology*, vol. 32, pp. 1868–1900, 2024, doi: 10.1016/j.jmrt.2024.08.018.

[4] The Aluminum Association, "Ford's All-Aluminum-Body F-150 Pickup Truck", 2021. [Online]. Available: https://www.aluminum.org [Accessed on 21 January 2025]

[5] G.A. Kunkel, and Y. Hovanski, "From the lab to your driveway: Aluminum tailor-welded blanks." *Welding Journal*, vol. 95 no. 8, pp. 36–39, 2016.

[6] Y. Hovanski, J. Carsley, B. Carlson, S. Hartfield-Wunsch *et al.*, "Comparing Laser Welding Technologies with Friction Stir Welding for Production of Aluminum Tailor-Welded Blanks." *SAE International Journal of Materials and Manufacturing*, vol. 7 no. 3, pp. 537–544, 2014, doi: 10.4271/2014-01-0791.

[7] F. Vollertsen and C. Thomy, "Welding with fiber lasers from 200 to 17000 W." *International Congress on Applications of Lasers & Electro-Optics*, pp 254-264, 2005, doi: 10.2351/1.5060499.

[8] S. Katayama, "Introduction: Fundamentals of laser welding," In *Handbook of Laser Welding Technologies*, Woodhead Publishing, Cambridge, UK, 2013, pp. 3–16.

[9] S.B. Chikalthankar, G.D. Belurkar, and V.M. Nandedkar, "Factors Affecting on Springback in Sheet Metal Bending: A Review." *International Journal of Engineering and Advanced Technology*, vol. 3 no. 4, pp. 247-251, 2014

[10] A.A. Zadpoor, J. Sinke, and R. Benedictus, "Springback behavior of friction stir welded tailor-made blanks," *Proceedings of the International Deep-drawing Research Group Conference 2007*, pp 317-324, 2007.

[11] T.B. Stoughton,"A general forming limit criterion for sheet metal forming". *International Journal of Mechanical Sciences*, vol. 42 no. 1, pp. 1–27, 2000, doi: https://doi.org/10.1016/S0020-7403(98)00113-1.

[12] M. Miles, "Formability Testing of Sheet Metals," in *Metalworking: Sheet Forming*, ASM International, Ohio, United States, 2006, pp. 673–696.

[13] J. Sinke, C. Iacono , and A.A. Zadpoor, "Tailor made blanks for the aerospace industry," *International Journal of Material Forming*, vol. 3, pp. 849–852, 2010.

[14] E. Ahmed, U. Reisgen, M. Schleser, and O. Mokrov, "On formability of tailor laser welded blanks of DP/TRIP steel sheets," *Science and Technology of Welding and Joining*, vol. 15 no.5, pp. 337–342, 2010, doi: 10.1179/136217110X12731414739754.

[15] L. Huang, X. Hua, D. Wu, and L. Fang, "Experimental Investigation and Numerical Study on the Elimination of Porosity in Aluminum Alloy Laser Welding and Laser–GMA Welding." *Journal of Materials Engineering and Performance,"* vol. 28 no. 3, pp.1618–1627, 2019.

[16] J. Wang, X. Chen, L. Yang, and G. Zhang, "A strength estimation method for aluminum alloy butt welded joints with mismatched mechanical properties," *Thin-walled Structures*, vol. 179, p. 109585, 2022, doi: 10.1016/j.tws.2022.109585

[17] J.M. Sánchez-Amaya, Z. Boukha, M.R. Amaya-Vázquez, L. González-Rovira, and F.J. Botana, "Analysis of the Laser Weldability under Conduction Regime of 2024, 5083, 6082 and 7075 Aluminium Alloys," *Materials Science Forum*, 713, pp. 7–12, 2012, doi: 10.4028/www.scientific.net/MSF.713.7.

[18] P. Sensharma, M. Collette, and J. Harrington, "Effect of welded properties on aluminum structures." S*hip Structure Committee*, 2010.

[19] M. Jiang, X. Chen, Y. Chen, and W. Tao, "Mitigation of porosity defects in fiber laser welding under low vacuum," *Journal of Materials Processing Technology*, vol. 276, 116385, 2020, doi: 10.1016/j.jmatprotec.2019.116385.

[20] H. Zhao, and T. DebRoy, "Macroporosity free aluminum alloy weldments through numerical simulation of keyhole mode laser welding," *Journal of Applied Physics*, vol. 93 no. 12, pp. 10089–10096, 2003.

[21] S. Katayama, M. Mizutani, and A. Matsunawa, "Development of porosity prevention procedures during laser welding," *Proc. SPIE 4831, First International Symposium on High-Power Laser Macroprocessing*, 3 March 2003, doi: 10.1117/12.497801.

[22] M. Miyagi, H. Wang, R. Yoshida, Y. Kawahito, H. Kawakami, and T. Shoubu, "Effect of alloy element on weld pool dynamics in laser welding of aluminum alloys,"*Scientific Reports*, vol. 8, 12944, 2018, doi: 10.1038/s41598-018-31350-4.

[23] R. Garcia, V. López, C. Natividad, R. Ambriz, and M. Salazar, "Fusion Welding with Indirect Electric Arc" in *Arc Welding*, InTechOpen, Rijeka, Croatia, 2011, pp 21- 44, doi: 10.5772/27113.

[24] S. S. Nayak, E. Biro, and Y. Zhou, “Laser welding of advanced high-strength steels (AHSS),” in *Welding and Joining of Advanced High Strength Steels (AHSS)*, Woodhead Publishing, Cambridge, UK, 2015, pp. 71–92.

[25] J. M Sánchez-Amaya, T. Delgado, J. J De Damborenea, V. Lopez, and F. J. Botana, “Laser welding of AA 5083 samples by high power diode laser,” *Science and Technology of Welding and Joining*, vol. 14 no. 1, pp. 78–86, 2009.

[26] Y. Zhang, F. Lu, H. Cui, Y. Cai, , S. Guo, and X. Tang, “Investigation on the effects of parameters on hot cracking and tensile shear strength of overlap joint in laser welding dissimilar Al alloys,” *The International Journal of Advanced Manufacturing Technology*, vol. 86, pp. 2895–2904, 2016.